



Belle II status and prospect *

Yoshiyuki Onuki

(On behalf of the Belle II Collaboration)

Department of Physics, The University of Tokyo, 7-3-1 Hongo, Bunkyo-ku, Tokyo, Japan
and

Systems Engineering and Science, Shibaura Institute of Technology, 307 Fukasaku, Minuma-ku, Saitama City, Saitama, Japan

Abstract

The Belle II experiment at the SuperKEKB accelerator is the upgraded successor of the B -factory, the Belle experiment and KEKB accelerator. The instantaneous luminosity is designed to $6 \times 10^{35} \text{ cm}^{-2}\text{s}^{-1}$ which is $30 \times$ higher than the KEKB. We aim to accumulate 50 ab^{-1} in the 2030 to discover a new physics beyond the Standard Model. The current integrated luminosity has reached 213 fb^{-1} in summer 2021. The Belle II can also provide various physics subjects: beauty, charm, τ -lepton, dark sector and hadron physics and etc. We confirm the detector performance as expected. Several physics results with leading precision have already been appeared. We briefly report the status and the prospect of the Belle II experiment.

Keywords: Super B -factory, Flavor physics, Beauty, Charm, τ , CKM, $\sin 2\phi_1$, $\sin 2\beta$, CP violation, BSM, ALPS, Z'

1. Introduction

It was proposed that the Origin of the Charge-Parity (CP) symmetry violation in the weak interaction is caused by an irreducible complex phase(s) in the flavor changing unitary matrix[1] in 1972. The B -meson was found to be a fertile place to study the CP violation mechanism in the early 80's[2] and an idea that the boosted B -meson system produced by asymmetric energy e^+e^- collider was proposed to verify experimentally. Two B -meson factories, BaBar and Belle experiments had been constructed in the 90's to verify the predicted large CP violation in the B -meson system. In 2002, the CP violation in the B meson system had been discovered by both experiments and verified. Because the cross sections of $\sigma(e^+e^- \rightarrow c\bar{c}) = 1.3 \text{ nb}$ and $\sigma(e^+e^- \rightarrow \tau^+\tau^-) = 0.9 \text{ nb}$ are comparable to the

$\sigma(e^+e^- \rightarrow \Upsilon(4S)) = 1.1 \text{ nb}$, the B -factories have another aspects both charm and τ factories. Many physical programs had been conducted by the B -factories over 20 years. Among them, discoveries in the exotic hadrons, such as heavy quarkonium-like X, Y and Z states, are notable achievements in the B -factories[3].

2. SuperKEKB accelerator and BelleII experiment

The Belle II experiment and SuperKEKB accelerator is the successor of the Belle experiment and KEKB accelerator to explore the physics beyond the Standard Model using a $50 \times$ larger statistics of that recorded by the Belle. The SuperKEKB accelerator adopts the nano beam scheme which can provide a $30 \times$ instantaneous luminosity of $6 \times 10^{35} \text{ cm}^{-2}\text{s}^{-1}$ [5]. The Belle II detector[4] is a multi purpose spectrometer composed of new sub-detectors as shown in Fig1: The innermost detector is the vertex detector(VXD) which consists of two inner layers of silicon pixel detector(PXD) and four outer layers of double-sided silicon strip detector(SVD). Tracking detector is 56 layers of drift wire

*Belle II status and prospect talk presented at QCD21, 24th International Conference in QCD (5-9/7/2021, Montpellier - FR).

Email address: yoshiyuki-onuki@g.ecc.u-tokyo.ac.jp
(Yoshiyuki Onuki
(On behalf of the Belle II Collaboration))

chamber(CDC). Two types of ring-imaging Cherenkov detectors for the particle identification detectors, time of propagation detector using quartz at the barrel region(TOP) and focusing aerogel RICH at the forward end-cap region(ARICH). CsI(Tl) crystals for the electromagnetic calorimeter surrounds the barrel and both the end-cap region. The super conducting magnet provides 1.5 T field and contained above detectors. The K_L and μ detector is composed of super-layers of iron sandwiched by resistive plate chamber or plastic scintillator detector(KLM). The front-end system of sub-detectors except for the PXD are in common DAQ framework. The trigger logic is made of combined information from CDC, TOP, ARICH, ECL and KLM within the $5 \mu\text{s}$ latency at maximum 30 kHz frequency. Obtained data from sub-detectors is merged to an event by the event builder PC farm. To reduce huge data from PXD, there is an extra feedback path in the PXD data acquisition to realize partial readout in the region of interest where the cross point of PXD surface and tracks interpolated by associated SVD and CDC hits. The raw data is stored at the KEK and the complete replica in the PNNL and the processing are performed in both. The data are distributed to the regional data center and processed by GRID sites in the world.

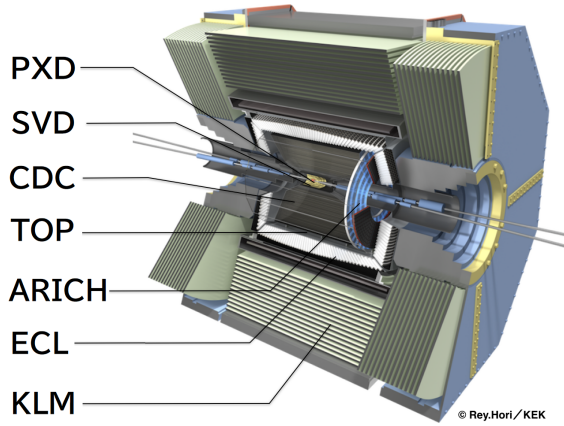


Figure 1: The Belle II detector.

The SuperKEKB accelerator is an asymmetric energy e^+e^- collider having a capability to scan the collision energy just below $\Upsilon(1S)$ to just above $\Upsilon(6S)$. For the $\Upsilon(4S)$ run, the beam energies are e^+ in 4GeV and the e^- in 7 GeV. The instantaneous luminosity L is provided by the formula

$$L = \frac{\gamma_{\pm}}{2er_e} \left(1 + \frac{\sigma_y^*}{\sigma_x^*}\right) \left(\frac{I_{\pm} \xi_{y\pm}}{\beta_y^*}\right) \left(\frac{R_L}{R_{\xi_{y\pm}}}\right), \quad (1)$$

where σ is the cross section, \pm denotes positron(+)-

electron(-) collider. The σ_{xy}^* is the beam size at the interaction point(IP) in the horizontal and vertical plane. I is the beam current, β_y^* is the vertical beta function at the IP, the $\xi_{y\pm}$ is the vertical beam-beam parameter, the R_L and $R_{\xi_{y\pm}}$ are the reduction factors for the luminosity and the beam-beam parameter, the r_e is the classical electron radius, and γ is the Lorentz factor. The nano-beam scheme strongly squeezes the β_y^* from 5.9 mm in the KEKB to 0.3 mm at the IP region. This is expected to increase $20 \times$ of the luminosity in the KEKB. Because keeping a low emittance is necessary in this scheme, new dumping ring for the positron injection was constructed and in operation since 2018. With a $1.5 \times$ increase of beam current, totally a $30 \times$ instantaneous luminosity is expected. The expected luminosity is shown in the Fig. 3. In the 2022, we will have a long shutdown(LS1) for the full installation of second PXD layers and exchange of TOP photomultitubes. In 2026, we are planning the LS2 for the IR upgrade for the full luminosity. By 2030, 50 ab^{-1} integrated luminosity is planned. The main goal of the Belle II experiment is to discover a phenomena of beyond the Standard Model and pointing to a new physics model. There are many promising and interesting modes which are summarized in [6] including τ , charm, hadron physics, dark sector and etc.

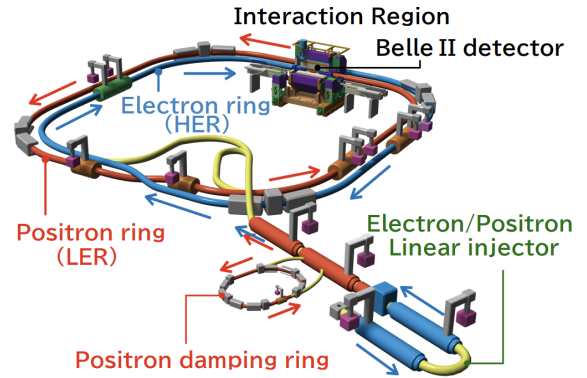


Figure 2: SuperKEKB accelerator.

3. Status of the Belle II experiment

SuperKEKB and Belle II project had started in 2012. In 2016, constructed SuperKEKB had started the commissioning. Beams only stored in both rings without collision and Belle II detector. After the success, Belle II detector without VXD was rolled in the IP region and pilot physics run(Phase-II) with beam collision had

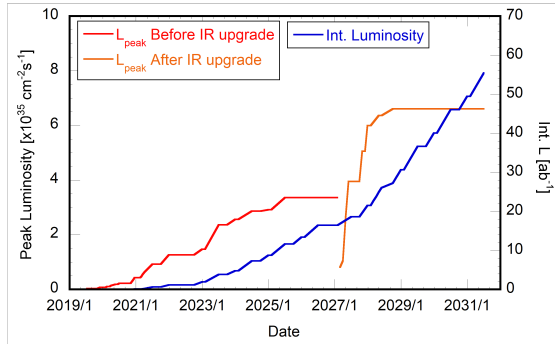


Figure 3: Luminosity projection in the next decade.

started in 2017. During the run, 472 pb^{-1} accumulated. In 2018, VXD was installed in the Belle II detector and the physics run had been started. Fig.4 shows the recorded physics data up to July-2021). In total, Belle II recorded 213.49 fb^{-1} physics data. The data taking efficiency of Belle II has reached $\sim 90\%$ in the latest operation. Also, SuperKEKB set a new world record of instantaneous luminosity $3.1 \times 10^{-34} \text{ cm}^{-2} \text{ s}^{-1}$ in end of the latest physics run (June-2021).

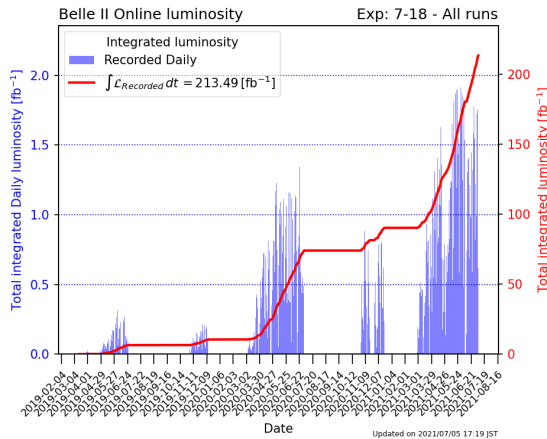


Figure 4: Recorded Belle II integrated luminosity in Phase III by July-2021.

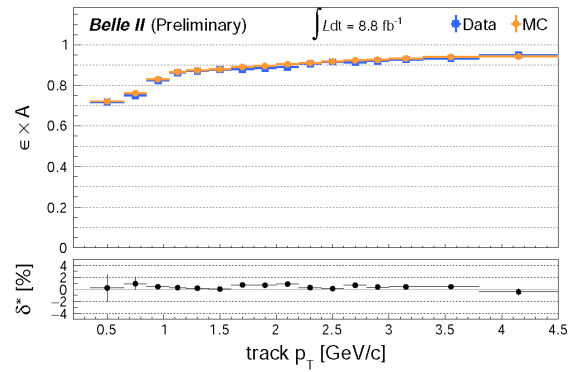
4. Detector performance

Evaluation of detector performance to deepen understanding of the detector is on-going using both real data and Monte Carlo simulation data (MC). In this section, we pick up important topics related to the later section.

The other notable feature, reconstruction of neutral particles at Belle II is given by [7].

4.1. Track efficiency

The tracking efficiency have been measured using $e^+e^- \rightarrow \tau^+\tau^-$ followed one τ decays 1-prong: $\tau \rightarrow \ell^+ \nu_\ell \bar{\nu}_\tau$, $\ell = e, \mu$ and the other decays 3-prong: $\tau \rightarrow 3\pi^+ \nu_\tau + n\pi^0$. In the reconstructed 1-prong τ decay, the fraction of 1 charge pion missing events to the decay is equivalent to a product of tracking efficiency ϵ and the detector acceptance A . The efficiency and the calibrated discrepancy δ^* between the data and MC are evaluated in terms of the transverse momentum of the 1-prong track as shown in Fig.5. The data and MC agreed well with small correction.

Figure 5: The measured product of tracking efficiency and detector acceptance with calibrated Data-MC inconsistency δ^* .

4.2. Particle identification

Particle identification (PID), is performed for each particle using the detected information from CDC, TOP, ARICH, ECL and KLM sub-detectors. These likelihoods are used to construct a combined likelihood ratio. The binary charged kaon/pion likelihood ratio can be defined by $\mathcal{R}_{K/\pi} = \mathcal{L}_K / (\mathcal{L}_K + \mathcal{L}_\pi)$. The PID performance was evaluated using $D^{*+} \rightarrow D^0 [K^-\pi^+] \pi^+$ decay using 37 fb^{-1} off-resonance (60 MeV below the $\Upsilon(4S)$) data and MC data [8]. The kaon identification efficiency ϵ_K is defined as: $\epsilon_K = (\text{number of kaon tracks identified as kaon}) / (\text{number of kaon tracks})$ while the pion mis-identification rate is defined as: $\pi \text{ mis-ID rate} = (\text{number of pion tracks identified as kaon}) / (\text{number of pion tracks})$. The Fig.6 shows the result of Kaon efficiency and pion mis-identification rate at the momentum.

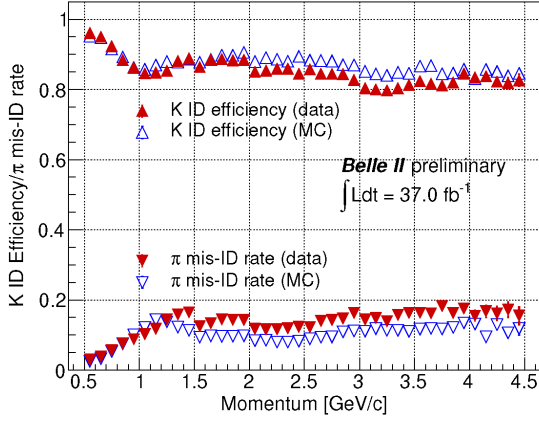


Figure 6: Kaon efficiency and pion mis-identification rate for the criterion $\mathcal{R}_{K/\pi} > 0.5$ using the decay $D^{*+} \rightarrow D^0[K^-\pi^+]\pi^+$.

4.3. Flavor tagging

In the time-dependent CP violation analysis, one of the two neutral B -mesons in mixing state is reconstructed in the specific CP eigenstate decay in interest. Flavor tagging is a determination of the other neutral B -meson(tag-side), B^0 or \bar{B}^0 , from the final state particles without reconstructing the decay. The algorithm is a necessary tool for the analysis and the high tagging efficiency is demanded. The flavor tagging algorithm using FastBDT is developed in Belle II[9]. The algorithm was trained by the flavor specific hadronic decays, $B^0 \rightarrow D^{(*)-}h^+(h = \pi, \rho, a)$ followed $D^{*-} \rightarrow \bar{D}^0\pi^-$, $D^- \rightarrow K^+\pi^-\pi^-, K_S\pi^-, K_S\pi^-\pi^0, K^+\pi^-\pi^-\pi^0$ and $\bar{D}^0 \rightarrow K^+\pi^-, K_S\pi^+\pi^-, K^+\pi^-\pi^0, K^+\pi^-\pi^+\pi^-$ using MC and the real data 8.7 fb^{-1} . The output of the algorithm is an index of the flavor tagging which defined by a product of flavor charge in $q = \pm 1$ and the dilution factor $r_{FBDT} \in [0, 1]$, where $q = +1/-1$ when B^0/\bar{B}^0 in tag-side, respectively. If one obtain the $q \cdot r_{FBDT} = 1$, the B -meson in tag-side is unambiguously B^0 . If one obtain the $q \cdot r_{FBDT} = 0$, the flavor is undetermined. The r_{FBDT} can be expressed $r_{FBDT} = 1 - 2w$, where w is the wrongly assigned flavor fraction. The Fig.7 shows the obtained $q \cdot r_{FBDT}$ distribution. The flavor tagging efficiency is estimated to be $(33.8 \pm 3.9)\%$ in comparison with $(30.1 \pm 0.4)\%$ in Belle.

5. Recent physics results

5.1. $\sin 2\phi_1$ measurement

Using 34.6 fb^{-1} , prompt measurement of time-dependent CP violation measurement and $B^0 - \bar{B}^0$ mixing measurement are conducted for the CP eigenstate

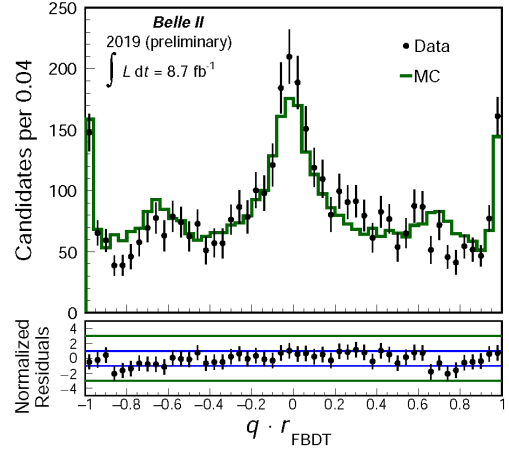


Figure 7: The $q \cdot r_{FBDT}$ distribution using $B^0 \rightarrow D^{(*)-}h^+$.

$B^0 \rightarrow J/\psi K_S$ decay and flavor specific $B^0 \rightarrow D^-\pi^+$ decay, respectively[10]. One B -meson is fully reconstructed as a signal decay. For the associated B -meson, the specific decay is not reconstructed but the decay vertex and the flavor information are reconstructed using the rest of tracks used for fully reconstructed B -meson. The distance between the vertexes of two B -mesons along with the boost direction of $\Upsilon(4S)$ can be convert to the proper-time interval Δt . The flavor in tag-side is determined by the flavor tagger in the previous Section 4.3. Using information of associated B -meson flavor, we can define the asymmetry

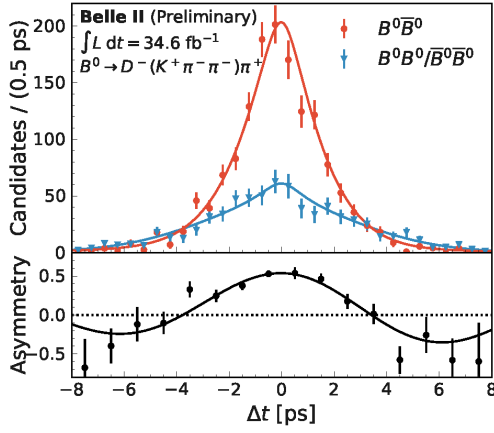
$$A_{mix}(\Delta t) \equiv \frac{N(B^0\bar{B}^0) - N(B^0B^0/\bar{B}^0\bar{B}^0)}{N(B^0\bar{B}^0) + N(B^0B^0/\bar{B}^0\bar{B}^0)} = (1 - 2w)\cos(\Delta m_d\Delta t) \quad (2)$$

where Δm_d is the mass difference of mixing and w is the wrong flavor tag fraction. Time-dependent mixing analysis is conducted using Eq.2 and Fig.8 shows the fit result of mixing and obtained $\Delta m_d = (0.531 \pm 0.046(stat) \pm 0.013(syst)) \text{ ps}^{-1}$.

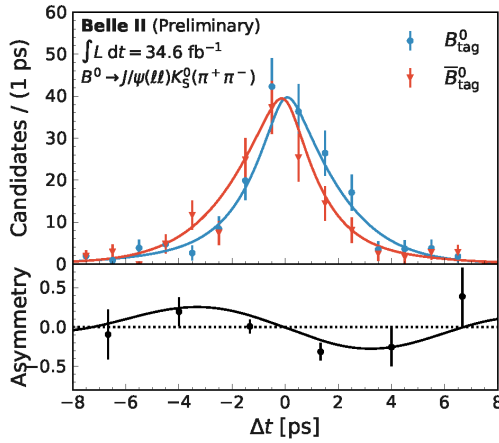
When we choose $B^0 \rightarrow J/\psi K_S$ in fully reconstruct decay, we can define the CP asymmetry

$$A_{CP}(\Delta t) \equiv \frac{N(\bar{B}^0_{tag}) - N(B^0_{tag})}{N(\bar{B}^0_{tag}) + N(B^0_{tag})} = S\sin(\Delta m_d\Delta t) + \mathcal{A}\cos(\Delta m_d\Delta t) \quad (3)$$

where Δm_d is the mass difference of mixing and w is the wrong flavor tag fraction, S is an indirect CP violation parameter stands for $S = \sin 2\phi_1$ and \mathcal{A} is a direct CP violation parameter which is assumed to be zero in this prompt analysis. We performed the time-dependent CP violation fit using Eq.3 for $B^0 \rightarrow J/\psi K_S$ as a probability density function convoluted with the proper-time resolution function obtained by the mixing study with $B^0 \rightarrow D^-\pi^+$. Fig.9 shows the fit result of CP violation measurement and we obtained $\sin 2\phi_1 =$

Figure 8: Δt distribution for reconstructed $B^0 \rightarrow D^- \pi^+$.

$0.55 \pm 0.21(stat) \pm 0.05(syst)$). Though the large statistical uncertainty, this result is consistent with the previous measurements.

Figure 9: Δt distribution for reconstructed $B^0 \rightarrow J/\psi K_S$.

5.2. Axion-like particle search

A pseudoscalar Axion-like particle (ALP) decaying into $\gamma\gamma$ is searched by Belle II using $445 \pm 3 \text{ pb}^{-1}$ [11]. The original Axion motivated by the strong CP problem but the ALP differs that the coupling constant is independent of the mass. The process, $e^+e^- \rightarrow \gamma a$ followed $a \rightarrow \gamma\gamma$, is used to look for the narrow axion peak in the squared invariant-mass $M_{\gamma\gamma}^2$ distribution and the squared recoiled-mass $M_{recoil}^2 = s - 2\sqrt{s}E_{recoil}^{c.m.}$ distribution. The signal yield fit is performed in the range $0.2 < m_a < 6.85 \text{ GeV}/c^2$ for the $M_{\gamma\gamma}^2$ and $6.85 < m_a < 9.8 \text{ GeV}/c^2$

for M_{recoil}^2 . The cross section can be calculated by the yield, and then it converts to the coupling constant ALP-photon $g_{a\gamma\gamma}$. The obtained 95% upper limit of $g_{a\gamma\gamma}$ is shown in Fig. 10. Using the initial data set, Belle II sets the most stringent constraint in $0.2 < m_a < 1 \text{ GeV}/c^2$ than the past experiments. Using increased luminosity, more than one order of magnitude improvement of $g_{a\gamma\gamma}$ sensitivity is expected in the future [12].

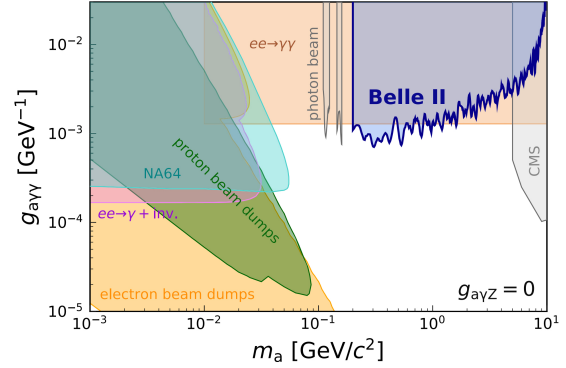


Figure 10: 95% C.L. upper limit of ALP-photon coupling.

5.3. Invisibly decaying Z' boson search

The recent $g - 2$ and $b \rightarrow s\ell^+\ell^-$ anomalies motivate an additional neutral boson in $L_\mu - L_\tau$ model [13] beyond SM. The BaBar experiment searched for the $e^+e^- \rightarrow \mu^+\mu^-Z'$ followed $Z' \rightarrow \mu^+\mu^-$ decay [14]. In the first time, Belle II reported both the process $e^+e^- \rightarrow \mu^+\mu^-Z'$ and lepton flavor violating $e^+e^- \rightarrow \mu^\pm e^\mp Z'$, and followed $Z' \rightarrow \text{invisible}$ decay using 276 pb^{-1} [15]. The search is conducting to find a peak of Z' invariant mass in the recoil against of $\mu^+\mu^-$ or $\mu^\pm e^\mp$ pair. Any excess is not found. The result is translated in the coupling constant of Z' in $L_\mu - L_\tau$ model and set the upper limit as shown in Fig. 11.

5.4. $B^+ \rightarrow K^+ \nu \bar{\nu}$ search using inclusive tagging method

The flavor-changing-neutral-current decay involves special interests in recent measurements of the $b \rightarrow s\ell^+\ell^-$ decays having tension to the SM. The $B^+ \rightarrow K^+ \nu \bar{\nu}$ also would provide a different probe of this issue and only lepton collider experiment would make it possible this measurement but not observed yet. The decay is experimentally challenging because nothing except for single charged kaon from the B -meson in reconstruction side. Hence, information of the B -meson in tag side, the partner of the B -meson in reconstruction side, must be used for the reconstruction. The branching fraction in

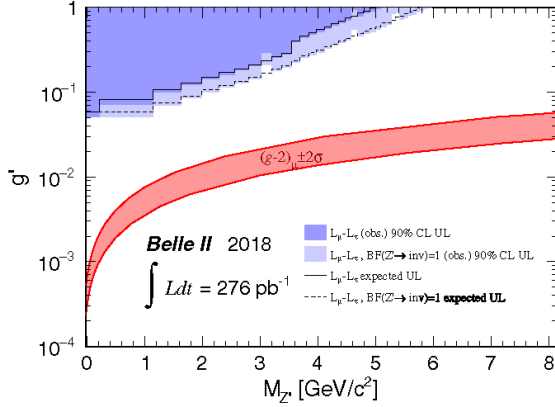


Figure 11: Upper limit of coupling constant g' with the favored band to explain the $g-2$ anomaly by the $L_\mu - L_\tau$ model (red).

SM prediction is $[4.6 \pm 0.5] \times 10^{-6}$ [16]. By BaBar and Belle, semi-leptonic and hadronic approaches of reconstruction in tag side were developed and applied for this mode and the variants[17–20].

A novel inclusive tagging method which doesn't assign the explicit decays of semi-leptonic and hadronic decay in the tag-side but exploits the decay topology and kinematics by BDT is developed. Using the inclusive tagging method and 63 fb^{-1} , Belle II reported the branching fraction $[1.9^{+1.3}_{-1.3}(\text{stat})^{+0.8}_{-0.7}(\text{syst})] \times 10^{-5}$ and set the upper limit 4.1×10^{-5} at 90% confidence level in this mode[21]. The result is almost comparable to both the results of Belle[18] and BaBar[19] using the hadronic tag based on the full dataset.

5.5. D^0 and D^+ lifetime measurements

D^0 and D^+ lifetimes are measured using $e^+e^- \rightarrow c\bar{c}$ events in 72 fb^{-1} data as in Fig.12[22]. The D^0 and D^+ are reconstructed by $D^0 \rightarrow K^-\pi^+$ and $D^+ \rightarrow K^-\pi^+\pi^+$ candidates from $D^{*+} \rightarrow D^0[K^-\pi^+]\pi^+$ and $D^{*+} \rightarrow D^+[K^-\pi^+\pi^+]\pi^0$ decays, respectively. Owing to the first layer of VXD is only 1.4 cm away from collision point in Belle II, the decay-time resolution is two times better than the Belle and BaBar experiments. These results, $\tau_{D^0} = 410.5 \pm 1.1(\text{stat}) \pm 0.8(\text{syst}) \text{ fs}$ and $\tau_{D^+} = 1030.4 \pm 4.7(\text{stat}) \pm 3.1(\text{syst}) \text{ fs}$, are the most precise result and consistent with the previous measurement[23].

5.6. Direct CP-violation in charmless $B \rightarrow K\pi$ decays.

The difference of direct CP-violation in the charmless $B \rightarrow K\pi$ decays, $\Delta\mathcal{A}_{K\pi} = \mathcal{A}_{K^+\pi^-} - \mathcal{A}_{K^+\pi^0} = 0.122 \pm 0.022$, had been observed to be nonzero which differs from the initial thought before the measurement

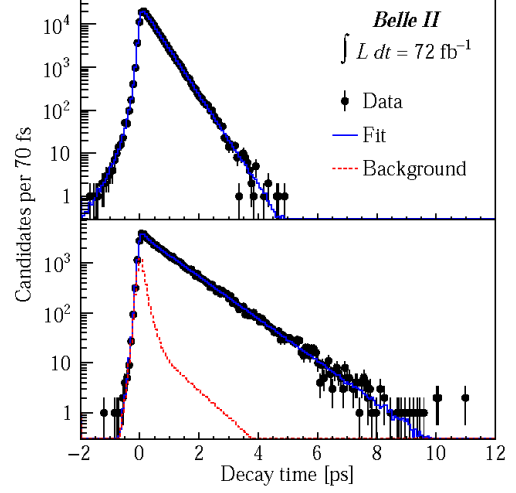


Figure 12: Decay-time distribution of $D^0 \rightarrow K^-\pi^+$ (top) and $D^+ \rightarrow K^-\pi^+\pi^+$ (bottom).

performed. This is known as $K\pi$ puzzle and regarded to be caused by hadronic effect if no NP contribution. The smoking gun test using isospin sum rule[24] was proposed by measuring the direct CP-violations and ratios of the branching fractions as in Eq.4

$$I_{K\pi} = \mathcal{A}_{K^+\pi^-} + \mathcal{A}_{K^0\pi^+} \frac{\mathcal{B}(K^0\pi^+) \tau_{B^0}}{\mathcal{B}(K^+\pi^-) \tau_{B^+}} - 2\mathcal{A}_{K^+\pi^0} \frac{\mathcal{B}(K^+\pi^0) \tau_{B^0}}{\mathcal{B}(K^+\pi^-) \tau_{B^+}} - 2\mathcal{A}_{K^0\pi^0} \frac{\mathcal{B}(K^0\pi^0)}{\mathcal{B}(K^+\pi^-)} = 0. \quad (4)$$

Especially, Belle II is expected to play an important role for the determination of the test in the modes including neutral particles K^0 and/or π^0 in the final state. The 62.8 fb^{-1} data is used for the analyses of $B^+ \rightarrow K^+\pi^0$ [26] and neutral $B^0 \rightarrow K^0\pi^0$ [25] which is the first analysis. The results are: $\mathcal{B}(K^+\pi^0) = [11.9^{+1.1}_{-1.0}(\text{stat}) \pm 1.6(\text{syst})] \times 10^{-6}$ and $\mathcal{A}_{K^+\pi^0} = 0.09 \pm 0.09(\text{stat}) \pm 0.03(\text{syst})$ [26], $\mathcal{B}(K^0\pi^0) = [8.5^{+1.7}_{-1.6}(\text{stat}) \pm 1.2(\text{syst})] \times 10^{-6}$ and $\mathcal{A}_{K^0\pi^0} = -0.40^{+0.46}_{-0.44}(\text{stat}) \pm 0.04(\text{syst})$ [25]. These are consistent with the previous measurement. Using the result with current world averages of the other experiments, $I_{K\pi} = -0.11 \pm 0.13$ is obtained. Belle II will determine the precision of $I_{K\pi}$ in the future because the $\mathcal{A}_{K^0\pi^0}$ precision dominates now and the precision will be reached a few % level at 50 ab^{-1} in 2030 in Fig.13.

6. Summary

The Belle II experiment covers very broad physics using the excellent detector and the large statistics. Some of the physics results shows already comparable or surpassing to the previous measurements in pre-

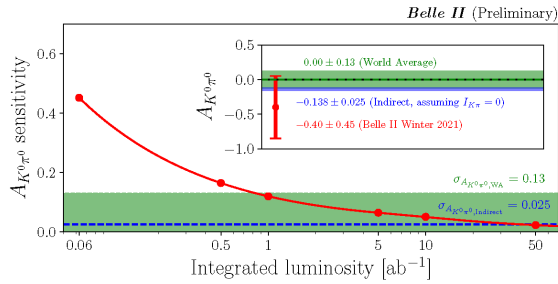


Figure 13: The projected sensitivity on $A_{K^0\pi^0}$.

cision in spite of the smaller data taken in the early stage. We are aiming to accumulate the luminosity 430 fb^{-1} comparable to the BaBar within this year. A lot of physics analysis is on going and the results leading in precision will be appeared soon.

References

- [1] N. Cabibbo, *Unitary Symmetry and Leptonic Decays*, *Phys. Rev. Lett.* **10**, 531 (1963); M. Kobayashi and T. Maskawa, *CP Violation in the Renormalizable Theory of Weak Interaction*, *Prog. Theor. Phys.* **49**, 652 (1973)
- [2] A. B. Carter and A. I. Sanda, *CP violation in B-meson decays*, *Phys. Rev. D* **23** 1567 (1981); I. I. Bigi and A. I. Sanda, *Notes on the Observability of CP Violations in B Decays*, *Nucl. Phys. B* **193**, 85 (1981)
- [3] A. J. Bevan et al., *The Physics of the B Factories*, *Eur. Phys. J. C.* (2014) 74:3026.
- [4] BelleII Technical Design Report. arXiv:1011.0352v1
- [5] Yuki Yoshi Ohnishi et al., Accelerator design at SuperKEKB, *Prog. Theor. Exp. Phys.* 2013, 03A011.
- [6] E. Kou et al., *The Belle II Physics Book*, *Prog. Theor. Exp. Phys.* **2019**, 123C01.
- [7] Belle II collaboration, $\pi^0 \rightarrow \gamma\gamma$ and $\eta \rightarrow \gamma\gamma$, BELLE2-NOTE-PL-2019-019; η and η' , BELLE2-NOTE-PL-2020-003; $K_S \rightarrow \pi^+\pi^-$, BELLE2-NOTE-PL-2018-016,
- [8] Belle II Collaboration, *Kaon and Pion Identification Performance in Phase III data*, BELLE2-NOTE-PL-2020-025,
- [9] Belle II Collaboration: F. Abudinén et al., *First flavor tagging calibration using 2019 Belle II data*, BELLE2-CONF-PH-2020-004, <https://arxiv.org/abs/2008.02707>
- [10] The Belle II Collaboration, *Prompt measurements of time-dependent CP-violation and mixing*, BELLE2-NOTE-PL-2020-011
- [11] F. Abudinén et al. (Belle II Collaboration), *Search for Axionlike Particles Produced in e^+e^- Collisions at Belle II*, *Phys. Rev. Lett.* **125**, 161806 (2020).
- [12] Matthew J. Dolan et al., Revised constraints and Belle II sensitivity for visible and invisible axion-like particles, *JHEP.* **94** (2017).
- [13] Wolfgang Altmannshofer et al., *Explaining dark matter and B decay anomalies with an $L_\mu - L_\tau$* , *JHEP.* **12**(2016) 106.
- [14] J. P. Lees et al. (BaBar Collaboration), *Search for a muonic dark force at BaBar*, *Phys. Rev. D* **94**, 011102(R) (2016).
- [15] I. Adachi et al. (Belle II Collaboration), *Search for an Invisible Decaying Z' Boson at Belle II in $e^+e^- \rightarrow \mu^+\mu^- (e^\pm\mu^\mp)$ Plus Missing Energy Final States*, *Phys. Rev. Lett.* **124**, 141801 (2020).
- [16] T. Blake, G. Lanfranchi, and D.M. Straub, *Rare decays as tests of the Standard Model*, *Prog. Part. Nucl. Phys.* **92** 50, (2017).
- [17] J. P. Lees et al. (BABAR Collaboration), *Search for $B \rightarrow K^{(*)}\nu\bar{\nu}$ and invisible quarkonium decays*, *Phys. Rev. D* **82** 112002, 2010.
- [18] O. Lutz et al. (Belle Collaboration), *Search for $B \rightarrow h^{(*)}\nu\bar{\nu}$ with the full Belle $\Upsilon(4S)$ data sample*, *Phys. Rev. D* **87** 111103(R), 2013.
- [19] J. P. Lees et al. (BABAR Collaboration), *Search for $B \rightarrow K^{(*)}\nu\bar{\nu}$ and invisible quarkonium decays*, *Phys. Rev. D* **87** 112005(R), 2013.
- [20] J. Grygier et al. (The Belle Collaboration), *Search for $B \rightarrow h\nu\bar{\nu}$ decays with semileptonic tagging at Belle*, *Phys. Rev. D* **96** 091101(R), 2017, erratum *Phys. Rev. D* **97** 099902 (2018).
- [21] Belle Collaboration: F. Abudinén et al., *Search for $B^+ \rightarrow K^+\nu\bar{\nu}$ decays using an inclusive tagging method at Belle II*, <https://arxiv.org/abs/2104.12624>
- [22] Belle II collaboration, Precise measurement of the D^0 and D^+ lifetimes at Belle II, submitted to *Phys. Rev. Lett.*; <https://arxiv.org/abs/2108.03216v1>,
- [23] P. A. Zyla et al. (Particle Data Group), *Review of Particle Physics*, *Prog. Theor. Exp. Phys.* **2020**, 083C01.

- [24] Michael Gronau, *A precise sum rule among four $B \rightarrow K\pi$ CP asymmetries.*, *Phys. Lett. B* **627** (2005) 82-88.
- [25] Belle II Collaboration: F. Abudinén et al., *First search for direct CP-violating asymmetry in $B^0 \rightarrow K^0\pi^0$ decays at Belle II*, <https://arxiv.org/abs/2104.14871>
- [26] F. Abudinén et al., *Measurement of branching fractions and direct CP-violating asymmetries in $B^+ \rightarrow K^+\pi^0$ and $\pi^+\pi^0$ decays using 2019 and 2020 Belle II data*, BELLE2-CONF-PH-2021-006, <https://arxiv.org/abs/2105.04111>